Molecular Cell
Article

Division of Labor between the Chromodomains of HP1 and Suv39 Methylase Enables Coordination of Heterochromatin Spread

Bassem Al-Sady,[1] Hiten D. Madhani,[1] and Geeta J. Narlikar[1,*]
[1]Department of Biochemistry and Biophysics, University of California, San Francisco, San Francisco, CA 94158, USA
*Correspondence: geeta.narlikar@ucsf.edu
http://dx.doi.org/10.1016/j.molcel.2013.06.013

SUMMARY

In *Schizosaccharomyces pombe*, heterochromatin spread, which is marked by histone 3 lysine 9 methylation (H3K9me), requires the chromodomains (CDs) of the H3K9 methylase Suv39/Clr4 and the HP1/Swi6 protein. It is unclear how the actions of these two H3K9me-recognizing CDs are coordinated. We find that the intrinsic preference of Suv39/Clr4 is to generate dimethylated H3K9 product. The recognition of pre-existing H3K9me marks by the CD of Suv39/Clr4 stimulates overall catalysis, enabling the accumulation of small amounts of trimethylated product in vivo. Coincidentally, the Suv39/Clr4 CD, unlike the HP1/Swi6 CD, has been shown to prefer the trimethyl state over the dimethyl state. We show that this preference enables efficient heterochromatin spread in vivo by reducing competition with HP1 proteins for the more prevalent dimethyl state. Our results reveal a strategy by which "writers" and "readers" of a chromatin mark exploit different methylation states on the same residue in order to facilitate collaboration and avoid competition.

INTRODUCTION

Constitutive heterochromatin is required for the long-term silencing of large stretches of the genome as well as for its structural integrity. This type of heterochromatin is signaled by methylation at lysine 9 of histone 3 (H3K9) and is conserved from *Schizosaccharomyces pombe* (*S. pombe*) to humans (Elgin and Grewal, 2003). The capacity of H3K9 methylation (H3K9me) and its associated silencing functions to initiate at specific DNA sequences and then spread beyond initiation sites in a sequence-indifferent manner is key to the normal function of constitutive heterochromatin (Grewal and Jia, 2007). Moreover, such spreading behavior can lead to the silencing of tumor suppressor genes and contribute to malignancy when heterochromatin is ectopically initiated in disease states (Bhalla, 2005; Carbone et al., 2006; Ceol et al., 2011; Reed-Inderbitzin et al., 2006).

The regulation of heterochromatin formation can be divided into initiation and spread steps. Initiation requires the recruitment of the SET domain H3K9 methylase "writer" enzyme to an initiation site. The initiation process has been extensively studied in *S. pombe*, wherein the H3K9me writer Suv39/Clr4 (Rea et al., 2000) exists in a protein complex called CLRC (Hong et al., 2005; Horn et al., 2005; Jia et al., 2005). Qualitatively distinct initiation mechanisms recruit either the Suv39/Clr4 methylase or the noncatalytic subunits of CLRC in order to trigger methylation (Bühler et al., 2007; Jia et al., 2004; Zofall et al., 2012). After initiation, H3K9me spreads via the combined action of the methylase and the two HP1 proteins, Swi6 and Chp2, and its extent is contained, in part, by the action of boundary elements (Noma et al., 2001).

Despite the central biological roles played by heterochromatin, the molecular mechanisms underlying its assembly and spread have remained opaque. One reason for the lack of mechanistic understanding is the combinatorial complexity of the process. H3K9me adopts three distinct states that can have distinct biological outputs: H3K9 monomethylation (H3K9me1), H3K9 dimethylation (H3K9me2), and H3K9 trimethylation (H3K9me3). In *S. pombe*, Suv39/Clr4 is the sole H3K9me writer, yet all three methylation states of H3K9 have been documented (Yamada et al., 2005). Therefore, the observed distribution of the H3K9me states either reflects the intrinsic activity of Suv39/Clr4 or is additionally regulated by other factors acting on this enzyme or its products. In metazoans, in contrast, different methylation states are achieved with different enzymes that can cooperate to generate specific H3K9me states (Cheutin et al., 2004; Fritsch et al., 2010; Peters et al., 2003; Rice et al., 2003; Tachibana et al., 2005). Adding to the combinatorial complexity is the participation of several heterochromatin proteins that recognize the H3K9me mark via a chromodomain (CD). The CDs of the HP1 proteins Swi6 and Chp2 recognize the H3K9me mark and coat heterochromatin to generate a platform that recruits diverse silencing regulators. Additionally, Swi6 is required for heterochromatin spread. At the same time, the N-terminal chromodomain (CD) of Suv39/Clr4 is also required for efficient spread of H3K9me and concomitant spread of CLRC (Noma et al., 2004; Zhang et al., 2008). This requirement has given rise to a feedback hypothesis whereby the recognition of the Suv39/Clr4 methylation product by its CD promotes further deposition of H3K9me.

These observations raise the following questions: (1) what is the mechanism of the positive feedback from the reaction product, and (2) how are the activities of the writer and reader CDs

coordinated to allow efficient spread rather than nonproductive competition?

Using a combination of biochemical dissection, a method we developed for comparing relative methylation levels at specific loci in vivo (Q-ChIP), and genetic approaches, we have uncovered a basic regulatory circuit that is coded within the intrinsic properties of Suv39/Clr4 and HP1/Swi6. We find that positive feedback from H3K9me enhances catalysis by Suv39/Clr4 in vitro and is required for the accumulation of the H3K9me3 state in vivo. Furthermore, we find that the previously documented selectivity of the Suv39/Clr4 CD for this modification state allows efficient heterochromatin spread by avoiding competition with HP1 proteins, which do not significantly distinguish between H3K9me3 and the more prevalent H3K9me2 states.

Our data uncover a division of labor strategy in heterochromatin formation wherein the recognition modules of writer and "reader" proteins are tuned to recognize distinct modification states of the heterochromatic mark, enabling productive collaboration between the two proteins.

RESULTS

First, to test proposals for the role of Suv39/Clr4 in the spread of H3K9me, we biochemically reconstituted an elemental reaction: H3K9me across an asymmetric dinucleosome with one nucleosome containing pre-existing H3K9me. Then, to study the cellular implications of the biochemical parameters identified by this approach, we developed a quantitative chromatin immunoprecipitation (ChIP) procedure termed Q-ChIP that utilizes external calibration with recombinant modified nucleosome standards to directly compare the amounts of H3K9me1, H3K9me2, and H3K9me3 formed in vivo. Then, using these approaches, we investigated the impact of CD specificity on spreading in vivo.

An H3K9me3 Mark Stimulates Suv39/Clr4 Catalysis, but Not Binding, on an Adjacent Nucleosome

First, we characterized the activity of Suv39/Clr4 on a mononucleosome in comparison to $H3_{1–20}$ peptide substrates using a fully recombinant system in which all components were bacterially expressed and purified. All reactions were performed under saturating concentrations of S-adenosyl methionine (Figure S2A available online). We found that Suv39/Clr4 displays increased catalytic specificity for nucleosomal substrates over tail peptides. This specificity most likely derived from a decreased K_M in the context of the nucleosome (Figure S1 and Supplemental Experimental Procedures). Then, we directly tested the prevalent hypothesis that pre-existing H3K9me marks enhance the activity of Suv39/Clr4 on chromatin by using a dinucleosome template (Figure 1A). The dinucleosome comprises one substrate nucleosome (N1) and one effector nucleosome (N2), which was either methylated at H3K9 with methyl-lysine analog (MLA) technology (Simon et al., 2007) or contained a nonmethylatable arginine at this position (K9R, Figure S2B). MLA substrates differ from unmodified substrates in that they harbor sulfur rather than carbon in the γ position of the lysine side chain (denoted as H3Kc9). This alteration can significantly affect the affinity of some CD-containing proteins (Munari et al., 2012; Seeliger et al., 2012). To assess whether the Suv39/Clr4 CD can efficiently recognize an MLA at H3K9, we compared the ability of H3Kc9me3 and H3K9me3 peptides to compete off fluorescently labeled H3K9me3 peptide bound to the Suv39/Clr4 CD. We found that the competitive abilities of H3Kc9me3 and H3K9me3 peptides are very similar, and their apparent K_I differed by only ~1.6-fold (Figure S3A). These results implied that the CD of Suv39/Clr4 recognizes an MLA at H3K9 with similar efficacy as a bona fide methyl mark.

We followed overall methyl incorporation by using a tritium (^{3}H)-labeled S-adenosyl methionine (SAM) methyl-donor tracer and saturating total SAM (Figure S2A). By measuring methylation at subsaturating concentrations of Suv39/Clr4, we obtained values for the specificity constant k_{cat}/K_M. The presence of a methyl mark on the adjacent nucleosome increased k_{cat}/K_M by ~5-fold (Figure 1C). This result validated the basic premise of the positive feedback model proposed for Suv39/Clr4 action (Elgin and Grewal, 2003; Hall et al., 2002; Zhang et al., 2008).

The increase in k_{cat}/K_M could reflect increased binding to the template or increased catalysis. If the increase is due to stronger binding of Suv39/Clr4 to the premethylated template, then k_{cat} would be the same for both substrates, and the K_M value would be lower for the premethylated substrate. We found that k_{cat} is ~4.3-fold faster for N1-$N2_{MLA}$ (0.021 min^{-1}) than N1-$N2_{K9R}$ (0.0049 min^{-1}) (Figures 1B and 1C) and recapitulates most of the stimulatory effect seen for k_{cat}/K_M. This suggests that the premethylated template increases catalysis, rather than binding, by the methylase. This conclusion was supported by our observation of similar K_M values for the two dinucleosome substrates (Figure 1C) (data not shown). Consistent with this conclusion, we found that Suv39/Clr4 binds H3Kc9me3 and H3K9 mononucleosomes with similar affinities when measured by electrophoretic mobility shift assays (Figure 1D; $K_{1/2}$ = 1.8 μM and1.5 μM for H3K9 and H3Kc9me3 nucleosomes, respectively). However, when binding is detected specifically proximal to the H3 tail with a fluorescence polarization assay, we find that the Suv39/Clr4-CD is capable of recognizing H3K9me on the mononucleosome (Figure 1E). We interpret these results to suggest that, similar to HP1/Swi6 (Canzio et al., 2011), Suv39/Clr4 interacts with the nucleosome in binding modes specific for H3K9me as well as alternative modes where the CD does not engage the methyl mark. The lack of obvious binding preference for methylated versus unmethylated nucleosomes when all binding events are measured indicates that alternative binding modes must dominate ground-state interactions of Suv39/Clr4 and the nucleosome. Altogether, these results indicate that the increased specificity for N1-$N2_{MLA}$ dinucleosomes derives primarily from a postbinding catalytic effect. To determine whether this effect in fact derives from CD engagement with MLA-installed H3K9me, we tested the impact of mutating the Suv39/Clr4 CD on catalysis. We find that the catalytic effect of H3Kc9me3 is indeed dependent on a functional Suv39/Clr4 CD (Figure S4C).

In principle, two models could account for the observed H3K9me3-dependent increase of the k_{cat}: (1) an allosteric and (2) a "guided state" model. In the allosteric model, when the Suv39/Clr4 CD is engaged at an H3K9me3 mark, it induces an allosteric change in the active site, directly increasing catalysis. In the guided state model, after initial substrate binding, the

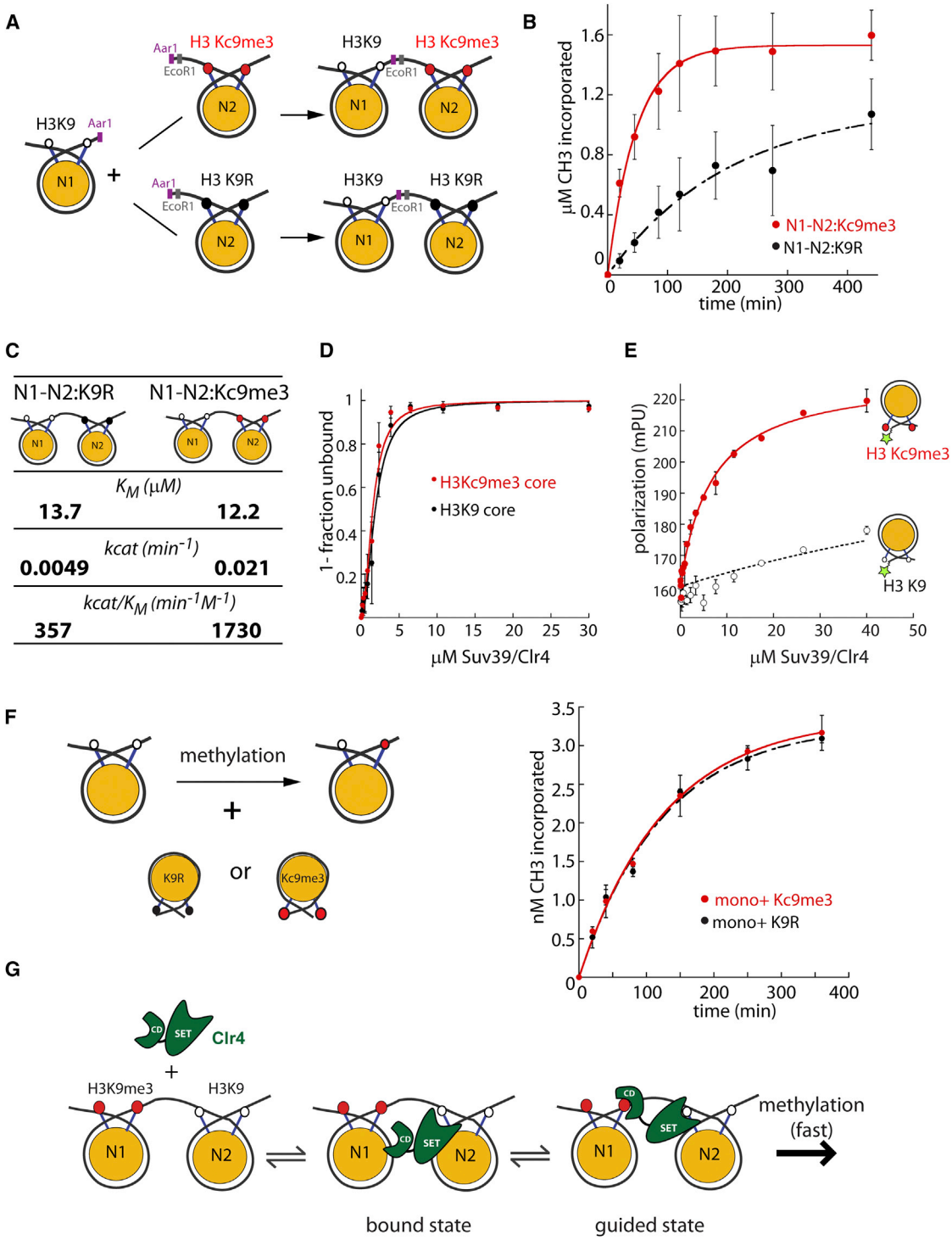

Figure 1. H3K9me3 Raises the k_{cat} of Suv39/Clr4 Only when Present In *cis* in a Dinucleosome Context

(A) A scheme for the production of asymmetric dinucleosomes.

(B) Dinucleosome methylation time courses at saturating (20 μM) Suv39/Clr4. For substrates, 100 nM N1-N2:K9R (black) or N1-N2:Kc9me3 dinucleosomes (red) were used. The k_{cat} values for Suv39/Clr4 for N1-N2:K9R and N1-N2:Kc9me3 were 0.0049 min^{-1} and 0.021 min^{-1}, respectively. The k_{cat} was derived from normalized data points from four separate experiments. Error bars denote the SE of four repeats.

(C) Enzymological parameters for Suv39/Clr4 activity on N1-N2:K9R or N1-N2:Kc9me3 dinucleosomes.

(D) Electrophoretic mobility shift experiments with H3K9 (black circles) and H3Kc9me3 (red circles) core mononucleosomes to determine the overall binding $K_{1/2}$. The $K_{1/2}$ of Suv39/Clr4 for H3K9 and H3Kc9me3 core mononucleosomes were 1.8 μM and 1.5 μM, respectively. Error bars denote the SE of three repeats.

(legend continued on next page)

CD-H3K9me3 interaction guides the Suv39/Clr4 active site so that it is properly oriented with respect to the substrate H3 tail. The allosteric model most simply predicts that the active site will be stimulated when the H3K9me3 mark is both in *cis* as well as in *trans* (not linked on the same substrate). In contrast, a guided state model would require the methyl mark to be present in *cis*. To test these predictions, we asked whether an H3Kc9me3-modified effector mononucleosome can stimulate the methylation of a substrate mononucleosome in *trans* in a methylation-sensitive manner. We performed these experiments at subsaturating concentrations of Suv39/Clr4 (Figures S1C and S1D) and with effector nucleosome concentrations above their $K_{1/2}$ values for binding Suv39/Clr4 (Figure 1D). In contrast to the behavior in *cis*, H3Kc9me3 effector mononucleosomes added in *trans* do not show greater stimulation than H3K9R effector nucleosomes (Figure 1F). We obtained similar results with peptide substrates or peptide effectors (Figures S2C and S2D).

The results from the above experiments argue against a simple allosteric mechanism for stimulation by the product (model 1). Instead, our results suggest that the H3K9me3 product acts in *cis* in a step subsequent to enzyme-substrate complex formation to stabilize a guided state that orients the Suv39/Clr4 active site with respect to the adjacent H3K9 substrate tail (model 2, Figure 1G).

Suv39/Clr4 Is a Preferential H3K9 Dimethylase of Nucleosomal Substrates

Unlike in metazoans, in *S. pombe*, all three H3K9me states are produced by one enzyme (Yamada et al., 2005). The ability of Suv39/Clr4 to produce all three methylation states is in part predicted from sequence homology of key active site residues to those of other H3K9me writers (Couture et al., 2008; Wu et al., 2010) and has been qualitatively demonstrated on peptide substrates (Dirk et al., 2007). However, the methylation state that is preferentially generated by Suv39/Clr4 on chromatin substrates is not known.

To determine the product distribution intrinsic to Suv39/Clr4, we measured the kinetics of H3K9me1, H3K9me2, and H3K9me3 on core mononucleosomes using saturating and excess Suv39/Clr4. We detected all three H3K9me states by western blot with antibodies raised to recognize the specific methylation state. Traditional western blot assays are limited in their quantitative resolution, hampering kinetic analysis. Therefore, we adapted a fluorescence-based system that allowed the measurement of methylation signals over a large dynamic range. The two fluorescence channels in this system allowed us to detect and quantify the H3K9me1, H3K9me2, or H3K9me3 signals and separately measure H4 levels for internally controlled normalization. As a standard for calibrating the western signals, we used histone octamers uniformly modified to be mono-, di-, or tri-methylated with MLA technology (Simon et al., 2007). The vendor-specified selectivity of antisera does not always match the observed specificity. Therefore, we experimentally quantified the selectivity of the three antisera used here (Figure S3B). For the most part, we found the antisera to be highly selective for the modification state they were raised against. In the case of the H3K9me2 antisera, we quantify about 10% cross-reactivity with H3K9me3.

The rate constant is defined as k_1 for the transition of unmethylated to monomethylated nucleosomes, k_2 for those from the mono- to di-methylated state, and k_3 for those from the di- to tri-methylated state (Figure 2A, top). Qualitatively, we observe a rapid rise and fall of H3K9me1, a gradual rise of H3K9me2, and a very slow rise of H3K9me3 (Figure 2A, bottom). The lags evident in H3K9me2 and H3K9me3 are expected from the consecutive nature of the methylation reactions. It is technically difficult to extract k_1, k_2, and k_3 from this type of time course data, given that the parameters are underdetermined in this setting. To overcome this limitation, we used MLA technology to produce intermediates of the overall reaction and used them as substrates to extract k_1, k_2, and k_3 for the subreactions in Figure 2A. To test the validity of using MLA substrates to mimic Suv39/Clr4 reaction intermediates, we compared the time courses for conversion of H3Kc9 nucleosomes to H3Kc9me2 nucleosomes with those for the conversion of H3K9 nucleosomes to H3K9me2 nucleosomes under the same conditions. We found that the two time courses essentially overlap (Figure S3C), indicating that H3K9 and H3Kc9 nucleosomes are equally good methylation substrates for Suv39/Clr4 and validating the use of these substrates for extracting individual rate constants.

First, we determined k_3 by measuring the rate of conversion of H3Kc9me2 to H3Kc9me3 nucleosomes with H3K9me3 antisera. Because this is a single conversion step, no lag was evident (Figure 2B, left), and the data could be fit to a single exponential, giving a k_3 of 0.0011 min^{-1}. This value is ~10-fold lower than the overall k_{cat}. To extract k_2, we measured the rate of H3Kc9me2 formation starting from H3Kc9me1 mononucleosomes. This allowed us to fit the data with a model containing the directly determined k_3 value, yielding a k_2 value of 0.011 min^{-1} (Figure 2B, middle). Finally, we determined k_1 by following H3K9me1

(E) Fluorescence polarization (FP) on nucleosomes. H3K9 (open black circles) and H3Kc9me3 (red circles) core mononucleosomes were fluorescently labeled at the 5′ end of the 147 bp positioning sequence. FP detected by this label is sensitive to local binding events, such as at the nearby H3 tail, as previously described (Canzio et al., 2011). The Suv39/Clr4 dependent FP increase at this position is at least 25-fold more sensitive to the presence of the H3Kc9me3 mark over the H3K9 control. In this panel, the bars shown do not denote the SE but, instead, show the variation between two independent repeats.

(F) Methylation of mononucleosomes in presence of effector nucleosomes in *trans*. Left, experimental design. Right, methylation time courses at 2 μM Suv39/Clr4 (below the K_M for di- and mono-nucleosomes). For substrates, 300 nM WT core mononucleosomes were used. K9R (black) or Kc9me3 core mononucleosomes (red) were added as effector in *trans* at 10 μM. In this panel, the bars shown do not denote the SE but, instead, show the variation between two independent repeats.

(G) A model for role of the Suv39/Clr4 CD in catalytic enhancement of H3K9me on chromatin. Formation of the enzyme-substrate ground state complex (bound state) is independent of pre-existing H3K9me marks. Catalysis requires the formation of a guided state, which optimally positions the active site relative to the H3K9 substrate. A pre-existing H3K9me mark stabilizes the guided state. The absence of a pre-existing H3K9me mark slows catalysis as the formation of the guided state is destabilized.

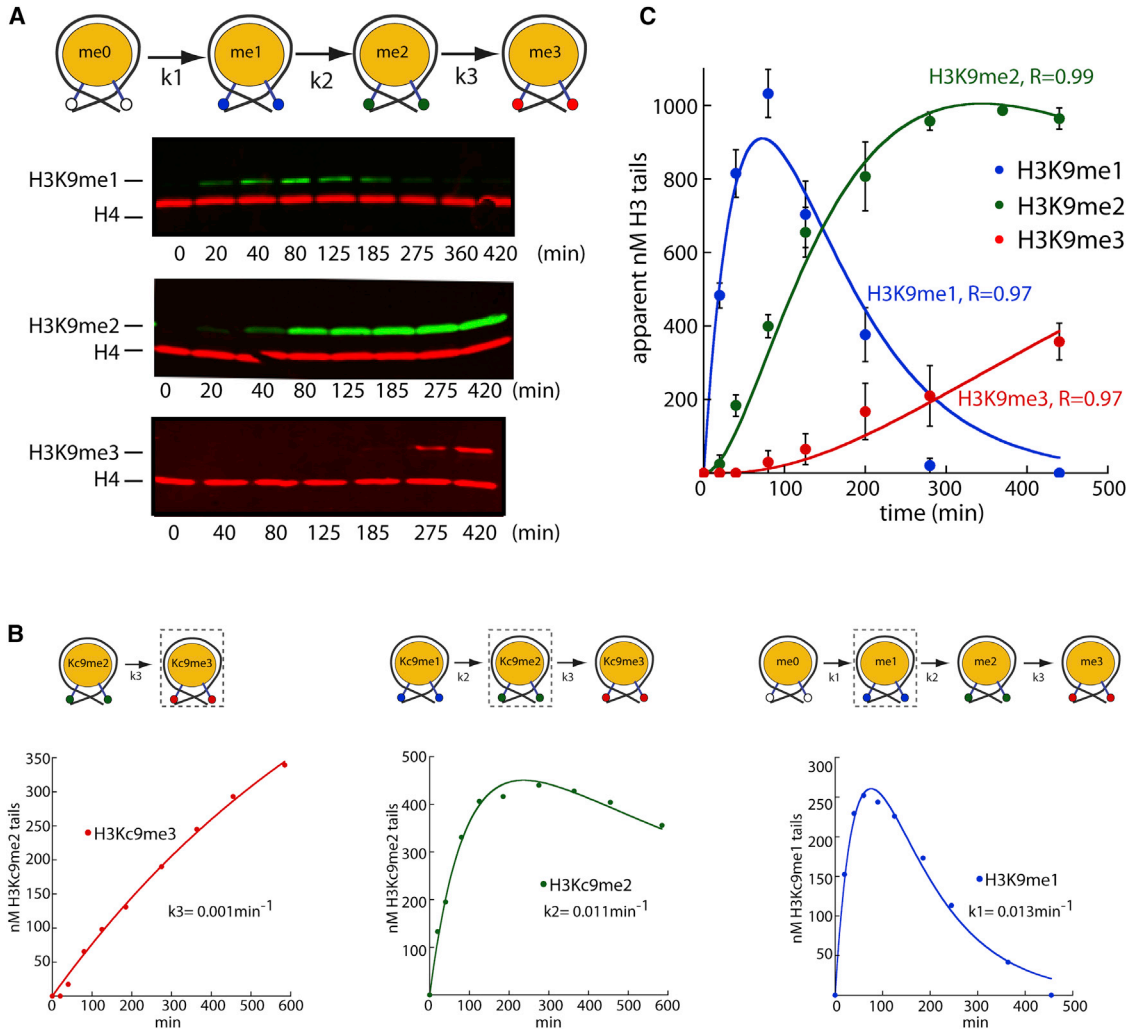

Figure 2. Suv39/Clr4 Is Primarily a H3K9 Dimethylase on Mononucleosomes

(A) Top, H3K9me by Suv39/Clr4 proceeds in a series of consecutive steps; e.g., monomethylation (k_1), dimethylation (k_2), and trimethylation (k_3). Bottom, quantitative western blots of H3K9me1, H3K9me2, and H3K9me3. Methylation reactions were performed at 20 μM Suv39/Clr4 and 125 nM core mononucleosomes. Reactions were stopped and separated by SDS-PAGE and probed for H4 (red) and H3K9me1 (green, top), H3K9me2 (green, middle), or H3K9me3 (red, bottom).

(B) Determination of k_1, k_2, and k_3. MLA core mononucleosomes representing intermediate steps of the consecutive reaction depicted in (A) were used as methylation substrates as in (A). The concentration of methylated tails in nanomolar (nM) is derived from the H4-adjusted amount of H3K9me1, H3Kc9me2, or H3Kc9me3 at each time point as determined by H3Kc9me1, H3Kc9me2, or H3Kc9me3 standards.

(C) Fitting the consecutive methylation reaction. k_1, k_2, and k_3 as determined from (B) were used to model the formation of H3K9me1, H3K9me2, and H3K9me3 starting from unmethylated core mononucleosomes. The lines describing the model fit well to the data obtained from unmethylated H3K9 nucleosomes. H3K9me1, H3K9me2, and H3K9me3 quantities determined as in (B).

Error bars denote the SE of three time courses.

formation using unmodified nucleosomes as the substrate. Fitting this data by a model containing the k_2 value determined as described above yielded a k_1 value of 0.013 min^{-1} (Figure 2B, right). In an additional validation of the above approach, a model with the k_1, k_2, and k_3 values fixed to the experimentally determined values recapitulates well the methylation time course on unmodified nucleosomes (Figure 2C; R = 0.97, 0.99, and 0.97 for mono-, di-, and tri-methylation, respectively).

Suv39/Clr4 displays almost identical k_1 and k_2 values, indicating that it does not distinguish unmethylated and monomethylated chromatin substrates. In contrast, k_3 is 10-fold lower than k_1 and k_2, indicating that dimethylated mononucleosomes are poor substrates for Suv39/Clr4. These results imply that the preferred product of Suv39/Clr4 is dimethylated H3K9.

H3K9me2 Is the Predominant Methylation State In Vivo

Next, we asked whether the in vitro preference for dimethylation was reflected in vivo. The H3K9me state distribution can be regulated by multiple factors in vivo, including, but not limited to, H3K9 demethylases. However, to date, the distribution of

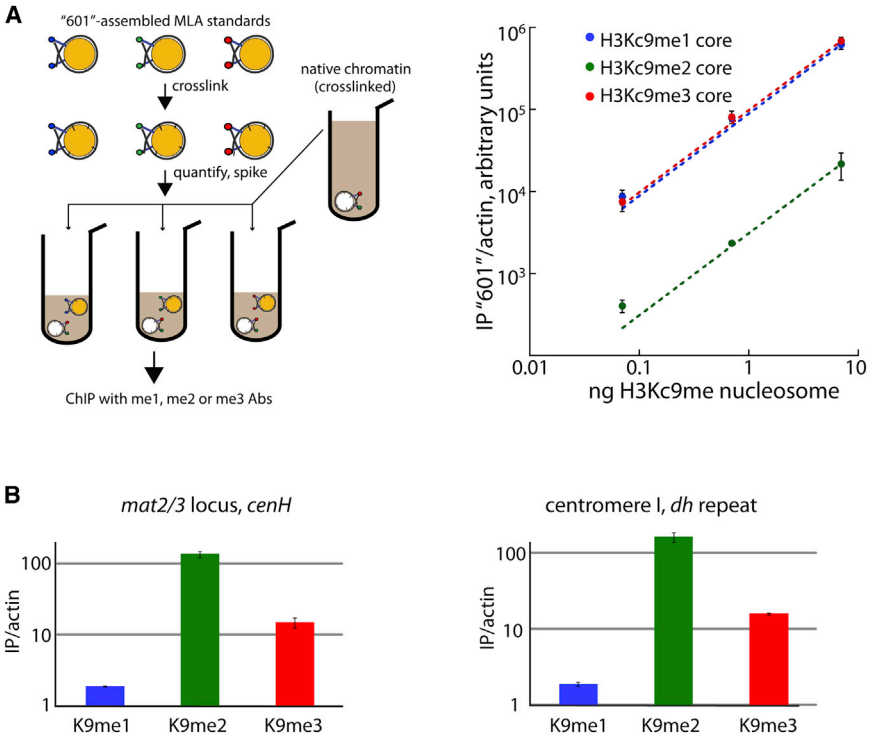

Figure 3. The Dimethyl State Is the Predominant H3K9me State In Vivo alongside a Small Trimethyl Pool

(A) The Q-ChIP method. Left, an overview of the H3Kc9me nucleosome ChIP spiking scheme. Right, a double log plot of the amount of cross-linked H3Kc9me1, H3Kc9me2, or H3Kc9me3 core mononucleosomes spiked into ChIP reactions (x axis) versus the amount of precipitated, actin-normalized 601 nucleosome DNA (y axis) as quantified by quantitative RT-PCR. Error bars denote the SE of three immunoprecipitations (IPs). (B) ChIP with H3K9me1 (blue), H3K9me2 (green), or H3K9me3 (red) antisera at the mating type locus *cenH* element (left) and the centromeric *dh* repeat (right). Enrichment is represented as the ratio of the actin-normalized signal in Suv39/Clr4 WT over the *clr4Δ* (no methylation) mutant. Relative H3K9me1, H3K9me2, and H3K9me3 signals were normalized by a parallel Q-ChIP reaction and are shown on a log scale. Error bars denote the SE of three IPs.

H3K9me states at specific heterochromatin loci has not been quantified. The primary tool for detecting different histone marks at specific loci is ChIP with highly specific ChIP antibodies (Peters et al., 2003). Given that the immunoprecipitation efficiency of antibodies varies widely, the amounts of the different histone marks cannot be directly compared. To enable a direct quantitative comparison between different methylation states in vivo, we developed Q-ChIP, a method of standardizing the ChIP signals deriving from H3K9me1, H3K9me2, and H3K9me3 antibodies (Figure 3A). We calibrated the ChIP externally by adding defined concentrations of H3Kc9me1, H3Kc9me2, and H3Kc9me3 core mononucleosomes assembled on the 601 sequence to the individual ChIP reactions. These concentrations spanned a 100-fold range. Calculating the amount of 601 DNA in the ChIP reactions allowed us to extract the relative efficiency of each antibody and normalize the ChIP signals for the three H3K9me states (Figure 3A).

Should the intrinsic catalytic capability of Suv39/Clr4 dominate the in vivo methylation profile, we would predict more H3K9me2 than H3K9me3 if the slower trimethylation reaction does not go all the way to completion. Indeed, using Q-ChIP at two primary heterochromatic loci, the centromeric *dh* repeat and the *cenH* initiation site of the silent mating type (*mat2/3*) region, we observed 1%–2% H3K9me1, ~84%–88% H3K9me2, and 10%–15% H3K9me3 (Figure 3B) (data not shown).

Product Guidance Is Required for the Maintenance of H3K9me3 Levels In Vivo

Next, we asked how product guidance impacts the distribution of H3K9me states produced by Suv39/Clr4. We adopted the quantitative western blot approach shown in Figure 2 using saturating concentrations of enzyme. To avoid interference from the H3Kc9me3 mark in the western blots, we biotin tagged the dinucleosome at the N1 end of the DNA, captured the N1-N2 substrate, and removed $N2_{MLA}$ or $N2_{K9R}$ by EcoRI cleavage prior to analysis by western blotting (Figure 4A). We observed that k_1, k_2, and k_3 were all elevated on N1-$N2_{MLA}$ versus N1-$N2_{K9R}$ (Figure 4B). The comparable increase of all three rates resulted in more H3K9me3 being produced on N1-$N2_{MLA}$ versus N1-$N2_{K9R}$ at the later time points. Given that H3K9me is a series of consecutive, irreversible reactions and that k_3 is the slowest rate, H3K9me3 levels were expected to be the most sensitive to disrupting product guidance.

To examine the role of product guidance in vivo, we mutated the critical W31 residue in the hydrophobic cage of the Suv39/Clr4 CD (W31A in this study). Such W31 mutants are not capable of recognizing H3K9me3 (Zhang et al., 2008) (Figure S4A) but are still capable of H3K9 methylation on peptides (Nakayama et al., 2001) (Figure S2C). Furthermore, we find that Suv39/$Clr4^{W31A}$ has similar H3K9me1, H3K9me2, and H3K9me3 rate constants on mononucleosomes as wild-type (WT) Suv39/Clr4 (Figure S4B), demonstrating that this CD mutant does not impact intrinsic methyltransferase activity. Consistent with previous observations (Noma et al., 2004), our Suv39/$Clr4^{W31A}$ mutant showed a significantly reduced spread of H3K9me outside the *cenH* initiation region of the *mat2/3* locus (data not shown). Then, we used Q-ChIP to investigate the relative distributions of H3K9me1, H3K9me2, and H3K9me3 at the centromeric *dh* repeat and the *cenH* initiation element in the Suv39/$Clr4^{W31A}$ mutant. We found that compromising product guidance results in a nearly complete loss of H3K9me3 at both those regions (Figure 4C) with much smaller effects on the other two methylation states. The H3K9me1 levels are increased 2-to 3-fold at both loci, whereas H3K9me2 is almost unaffected. These results are consistent with the predictions from the biochemical analysis in Figure 4B.

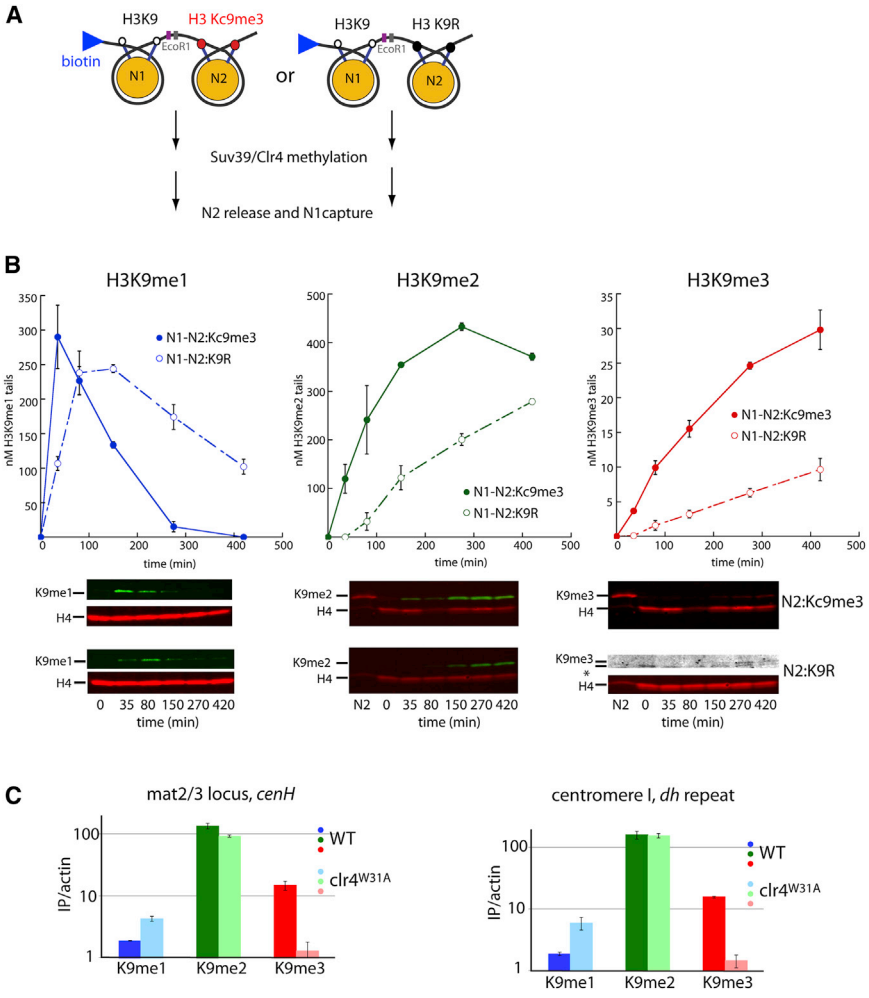

Figure 4. Impact of Product Guidance on H3K9me3 Accumulation In Vitro and In Vivo

(A) A scheme for measuring mono-, di-, and trimethylation on biotin-N1-$N2_{K9R}$ and biotin-N1-$N2_{MLA}$ dinucleosomes. Methylation reactions were performed as in Figure 2A, and reactions were stopped with 2 mM SAH. After reactions, N2 effector nucleosomes were released by EcoRI restriction digestion, and N1 nucleosomes were separated by SDS-PAGE and probed with indicated antisera.

(B) Top, quantification of western blot data as in Figure 2B. Bottom, representative western blots. N2 represents effector nucleosomes from the t = 0 min time point. The N1-N2:K9R anti-H3K9me3 blot is enhanced to show the very small pool of detectable H3K9me3. Error bars denote the SE of three time courses.

(C) The Suv39/Clr4 W31A mutation leads to a loss of H3K9me3 at the *mat2/3* locus *cenH* element or centromere *dh* repeat. Q-ChIP was performed as in Figure 3B. The Suv39/$Clr4^{W31A}$ is denoted in light colors. WT data are the same as in Figure 3B and are shown for comparison. Error bars denote the SE of three IPs.

The H3K9me3 Selectivity of the Suv39/Clr4 CD Is Required for Spread and Prevention of Nonproductive Competition

In trying to understand the significance of the H3K9me state distribution in vivo and its relation to spreading, we recalled prior studies that have shown that the CD of Suv39/Clr4 is unique among the CDs of heterochromatin factors in *S. pombe* in its H3K9me state selectivity. The HP1 proteins Swi6 and Chp2 and the RITS-associated Chp1 protein have CDs that discriminate only 1.5- to 2-fold between H3K9me3 over H3K9me2 (Fischle et al., 2003; Sadaie et al., 2008; Schalch et al., 2009; Yamada et al., 2005), whereas the CD of Suv39/Clr4 has a 5- to 6-fold preference for H3K9me3 over H3K9me2 (Schalch et al., 2009; Zhang et al., 2008). This selectivity of the Clr4 CD is comparable to the selectivities of H3K4me3-specific plant homeodomain finger factors (Li et al., 2006; Peña et al., 2006). We tested whether this difference had a functional impact on the spread of H3K9me.

We swapped the CD of Suv39/Clr4 with that of Chp1 mutated at F61 to alanine ($Chp1CD^{F61A}$). This mutation yielded a similar affinity for H3K9me3 as the WT CD of Suv39/Clr4 but exhibited a 3-fold tighter affinity for H3K9me2 (Schalch et al., 2009), effectively reducing the selectivity of Suv39/Clr4 for H3K9me3. We find that $Clr4^{chp1CDF61A}$ rescues the silencing function of Suv39/Clr4 at an ectopic locus, unlike the CD functional null Suv39/$Clr4^{W31A}$ (Figure S5B). However, although the distribution of H3K9me states in $Clr4^{chp1CDF61A}$ at endogenous initiation sites is similar to WT Suv39/Clr4 (Figures 5B and S5C), the spread of methylation beyond presumptive initiation sites (*cenH* and *REIII*) in the *mat2/3*-silenced region is dramatically reduced (Figure 5C), albeit not abolished, as in Suv39/$Clr4^{W31A}$.

Given that we converted the CD of Suv39/Clr4 into one that could, in principle, compete better with the CDs of HP1 proteins for H3K9me2 and that HP1 proteins are required for the spread of heterochromatin (Hall et al., 2002; Kanoh et al., 2005), we hypothesized that the displacement of HP1 proteins by the engineered CD might account for part of the defect in heterochromatin spread. Consistent with this notion, we observed that HP1/Swi6 levels at the centromeric *dh* repeat or the *cenH* initiation element are reduced ~2-fold in the mutant (Figure 5D), even though overall H3K9me is not significantly altered at these sites (Figures 5B and S5C). Additionally, the HP1 protein Chp2 is reduced to a similar extent at the mating-type locus *cenH* initiation site, whereas it is only mildly decreased at the centromeric *dh* element (Figure 5E). These results demonstrate that the binding preference of the CD of Suv39/Clr4 for the trimethylated state of H3K9 is critical for the lateral spread of heterochromatin in vivo, we hypothesize, in part because it reduces nonproductive competition with HP1 proteins (see Discussion).

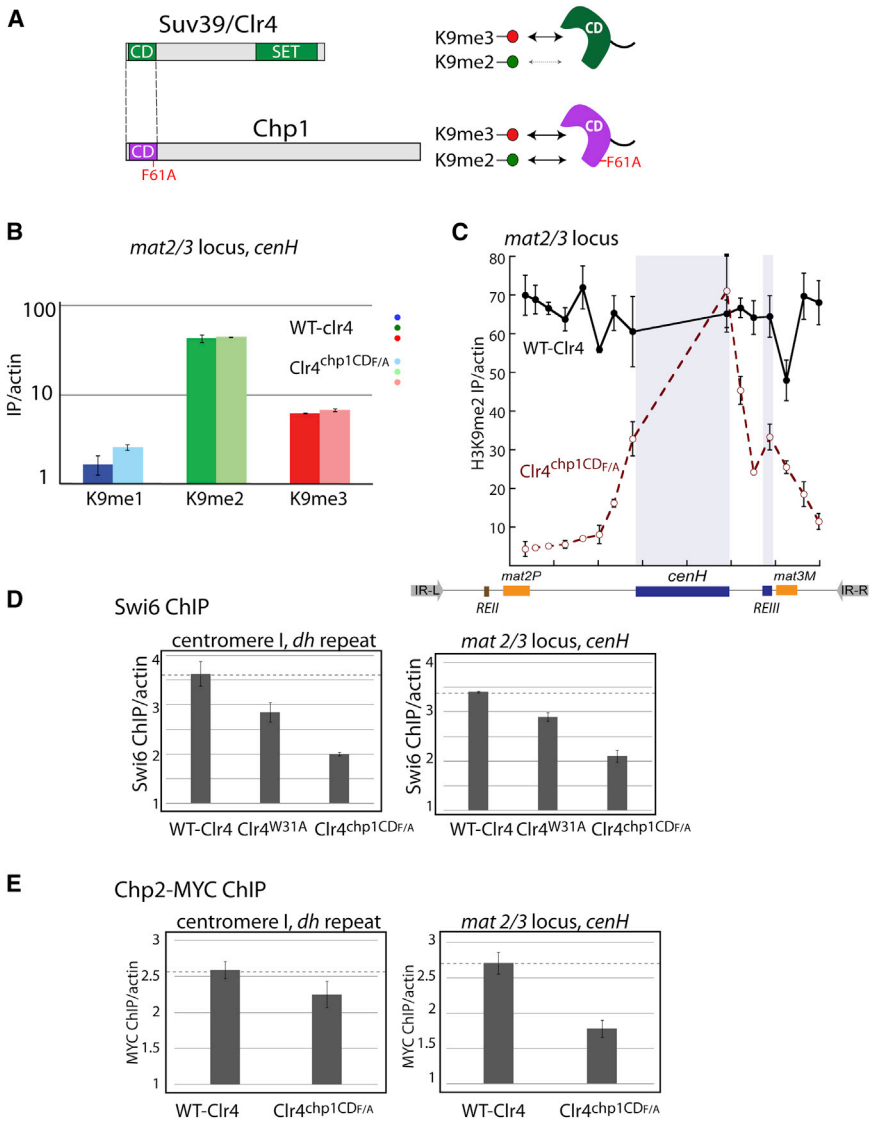

Figure 5. Impact of Changing H3K9me3 Selectivity of the Suv39/Clr4 CD on Methylation Spread and HP1 Assembly in Vivo

(A) The CD of Suv39/Clr4 (residues 1–64) was swapped for the F61A mutant CD of Chp1 (1–77). The F61A Chp1 CD has a similar preference for H3K9me2 and H3K9me3, whereas the Clr4 CD is more H3K9me3 specific.

(B) H3K9me1, H3K9me2, or H3K9me3 signals in Suv39/Clr4 WT or Suv39/Clr4^{chp1CDF61A} at the *cenH* initiation region probe of the *mat2/3* locus were quantified as in Figure 3B.

(C) H3K9me2 signals across the *mat2/3* locus in Suv39/Clr4 WT or Suv39/Clr4^{chp1CDF61A} backgrounds.

(D) The Suv39/Clr4^{chp1CDF61A} CD domain swap decreases HP1/Swi6 at initiation sites. Swi6 enrichment over a *clr4Δ* mutant normalized to an actin control is shown.

(E) The Suv39/Clr4^{chp1CDF61A} CD domain swap decreases Chp2:7xMYC at the *mat2/3* locus and, to a lesser degree, at the centromere. Chp2:7xMYC enrichment over a *clr4Δ* mutant normalized to an actin control is shown.

Error bars represent the SE of three IPs.

DISCUSSION

In *S. pombe*, the spread of heterochromatin relies on the recognition of H3K9me marks by both readers as well as the enzymatic writers that put on the mark. Two central questions emerge from this arrangement: (1) how does the recognition of the writer reaction product, H3K9me, regulate Suv39/Clr4 to promote spread, and (2) how do readers and writers coordinate H3K9me recognition through their respective CDs to avoid nonproductive competition for this mark? We find that a key to answering these questions lies in the central finding presented here that different modification states of the same chromatin mark, in this case H3K9me2 and H3K9me3, take on distinct roles.

Catalytic Stimulation Underlies Positive Feedback by the Suv39/Clr4 Product

The finding that H3K9me recognition modules in writer and reader proteins are required for heterochromatin spread has led to a positive feedback hypothesis wherein it is postulated that pre-existing methylation events help stimulate subsequent rounds of H3K9me. The mechanistic basis of such feedback is not fully understood. Two broadly recognized classes of mechanisms have been proposed for how a mark might promote its own formation via a reader-writer protein-enhanced binding or allosteric activation. We find that H3K9me3, present on both tails in *cis* on a neighboring nucleosome, stimulates catalysis by Suv39/Clr4 rather than by substrate binding. Furthermore, we exclude a straightforward allosteric mechanism (Figures 1F, S2C, and S2D). The stimulatory effect is most simply accounted for by a model in which the CD:H3K9me3 interaction guides the correct alignment of the substrate reactive groups relative to the active site residues. In such a model, the CD:H3K9me3 interaction occurs after binding to stabilize a high-energy guided state in which the H3 tails of the adjacent nucleosome are optimally positioned within the SET domain active site (Figure 1G). In principle, the guiding nucleosome can be methylated on one or both (as in our experiments) tails. If the formation of a guided state were highly sensitive to the steric arrangement of methylated tail and substrate, then a nucleosome methylated on one tail would exercise guidance only if such constraints were satisfied. Alternatively, should guidance not be sensitive to whichever of the two effector nucleosome tails is methylated, singly methylated nucleosomes would be at least 2-fold less efficient at catalytic stimulation, and full stimulation would require the methylation of both tails.

The formation of the guided state will most likely rely on a conformational change within Suv39/Clr4 following initial engagement with the nucleosome. Narrowly interpreted, this model would predict that binding of Suv39/Clr4 to chromatin in vivo should not depend on its CD. However, ChIP experiments, a proxy for binding in vivo, indicate that CLRC components localize specifically to heterochromatic regions in a manner dependent on the Suv39/Clr4 CD (Zhang et al., 2008). Therefore, it is likely that other subunits of the CLRC complex, or other regulators, recognize features of heterochromatin (e.g., bound HP1/Swi6) to further stabilize the high-energy guided state of Suv39/Clr4, resulting in CD-dependent ChIP of CLRC components.

Regulation from the reaction product is common in chromatin biology (Kirmizis et al., 2007; Lan et al., 2007; Margueron et al., 2009) and has been extensively analyzed in the context of H3K27 methylation by the PRC2 complex (Margueron et al., 2009). In this case, there is strong evidence for canonical allosteric activation, given that the product peptide provided in *trans* stimulates methylation by the catalytic EZH2 subunit (Margueron et al., 2009). In contrast to this type of mechanism, guided-state-based mechanisms require activators in *cis* and may allow enzymes such as Suv39/Clr4 to integrate specificity determinants distributed over a complex substrate, such as a dinucleosome. Analogous postbinding catalytic effects of enzymatic residues that are distant from the active site have been documented in other enzymatic systems (Narlikar and Herschlag, 1998, reviewed in Jencks, 1987).

The Product Guidance Mechanism Is Required for the Accumulation of H3K9me3 In Vivo

In vitro, the absence of a product guidance mark lowers the rates for generating each methylation state. Given that H3K9me3 is the terminal product, there is a large cumulative impact on H3K9me3 levels at any given time (Figure 4B). Consistent with these in vitro observations, compromising product guidance in vivo leads to a severe reduction in H3K9me3 at presumptive initiation sites (Figure 4C). Previous work has shown that compromising the ability of the Suv39/Clr4 CD to recognize the H3K9 methyl mark greatly diminishes H3K9me spread beyond the initiation sites (Noma et al., 2004). Our data raise the possibility that the lack of spread observed previously is mechanistically related to the reduction in H3K9me3 levels at the initiation sites. We discuss this possibility further in the next section (Figure 6).

Division of Labor between the Chromodomains of HP1 and Suv39/Clr4 Is Required for Productive Heterochromatin Assembly

We find that the distribution of H3K9me states catalyzed by Suv39/Clr4 is critical for allowing H3K9me spread and for avoiding nonproductive competition with the two central *S. pombe* HP1 proteins, Swi6 and Chp2. Our in vitro measurements show that the formation of H3K9me3 from H3K9me2 is 10-fold slower than the formation of either H3K9me2 or H3K9me1 (Figure 2). Correspondingly, using a quantitative method that we developed to measure individual methylation states, we find that cellular levels of H3K9me3 are ~10-fold lower than H3K9me2 levels in vivo (Figure 3). At the same time, our results with the Suv39/Clr4 CD mutant indicated that the spread of methylation is correlated with the presence of the trimethyl state in the initiation sites (Figures 4B and 4C). Why then are the H3K9me3 levels maintained at a low level in vivo? We believe the different levels of H3K9me3 and H3K9me2 reflect the need to separate the role of H3K9me3 in regulating Suv39/Clr4 spread from the role of H3K9me2 in directing structural assembly by HP1 proteins.

In support of the above hypothesis, we found that selective recognition of the Suv39/Clr4 CD for the trimethylated state of H3K9 is required for the spread of heterochromatin in vivo (Figure 5C). Suv39/Clr4 has a higher preference for the H3K9me3 mark than the *S. pombe* HP1 proteins (Nakayama et al., 2000; Schalch et al., 2009; Zhang et al., 2008). Engineering the Suv39/Clr4 CD to increase its affinity for the dimethyl state while maintaining the same affinity for the trimethyl state (Figure 5A) results in a significant loss of H3K9me spread (Figure 5B). Importantly, this increase in selectivity for the dimethyl state results in a reduction in the recruitment of the HP1 proteins Swi6 and Chp2 at initiation loci (Figures 5D and 5E). The simplest explanation for this reduced recruitment is that the engineered Suv39/Clr4 protein is now better at competing with HP1 proteins for binding to H3K9me2. Such a competitive scenario requires H3K9me reader proteins to be present in excess of H3K9me binding sites so that H3K9me tails are, in fact, limiting. This is broadly consistent with the published data, which indicate that HP1/Swi6 accumulates to about 20,000 copies per cell (Sadaie et al., 2008). This represents about a 10-fold excess over H3K9me tails that participate in heterochromatin initiating regions (~120 kb). Altogether, these results provide a biological rationale for why Suv39/Clr4 prefers to generate H3K9me2 over H3K9me3.

Altogether, our data suggest a model in which the small cellular H3K9me3 pool plays roles in spreading while the dominant H3K9me2 pool plays roles in assembly (Figure 6). At initiation sites, the recruitment of Suv39/Clr4 mostly leads to local H3K9me2 and small amounts of H3K9me3. We hypothesize that the CD of Suv39/Clr4 primarily engages the H3K9me3 mark. This leaves the predominant H3K9me2 species free to be bound by the CDs of HP1 proteins, which do not distinguish significantly between the H3K9me2 and H3K9me3 states. When Suv39/Clr4 encounters an available H3K9me3 nucleosome, the methylation of adjacent unmethylated nucleosomes is stimulated. We speculate that the HP1 protein Swi6 is nonredundantly required for spread at the *mat2/3* locus by masking previously methylated regions and preventing Suv39/Clr4 from getting trapped in these methylated regions.

Overall, our data reveal strategies that allow writer enzymes and reader proteins to productively engage in the formation of a heterochromatic domain. This is accomplished in two ways; first, the affinities of the chromatin-mark-binding modules are tuned differentially such that writers and readers are sensitive to different modification states. Second, the writer enzyme has access to one of the modification states, and this state stimulates the writer enzyme on the chromatin template to achieve enhanced catalysis dependent on proximity to previously deposited reaction products. Altogether, these two strategies allow for the productive collaboration between reader and writer proteins in the spread of a chromatin mark.

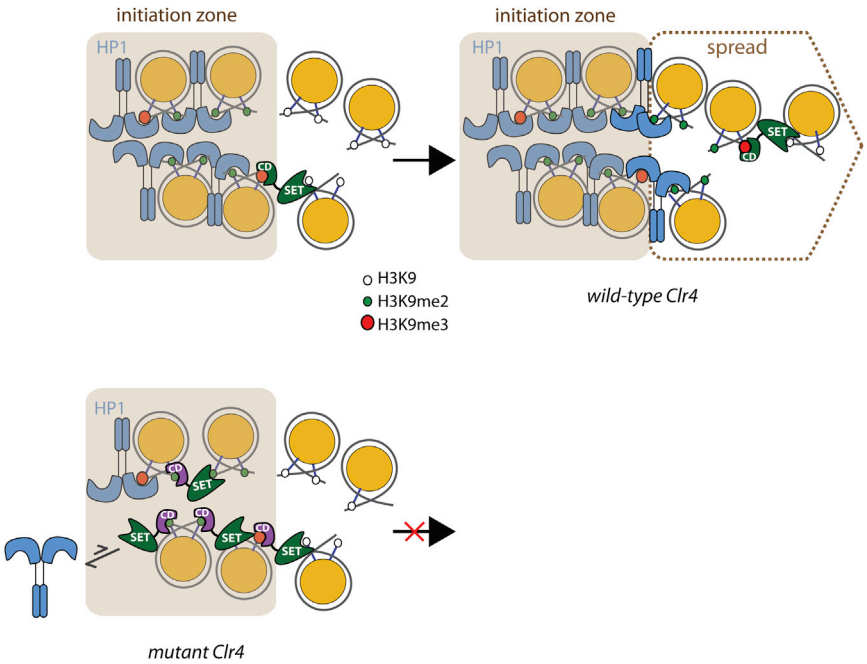

Figure 6. Model for the Coordination of Suv39/Clr4 and HP1 Protein Chromodomains in H3K9me Spread across Nucleosomes

In the initiation zone, a pool of H3K9me2 and H3K9me3 marks is formed by directly recruited Suv39/Clr4 molecules. The CDs of HP1 proteins such as Swi6 and Chp2 cover most of the central H3K9me2 and H3K9me3 marks. Specific H3K9me2 and H3K9me3 recognition of some HP1 proteins such as Swi6 requires oligomerization mediated by the chromatin template (Canzio et al., 2011), exposing H3K9me2 and H3K9me3 at the edge of the heterochromatic domain. In the context of the WT enzyme, exposed H3K9me3 marks act as a guidance mark for Suv39/Clr4. Any nearby unmethylated nucleosome transiently available for the guided state of Suv39/Clr4 will be methylated, resulting in H3K9me2 and a small H3K9me3 pool. These new sites are covered by the HP1 proteins, preferentially exposing H3K9me tails at the edge of the growing heterochromatin structure. Suv39/Clr4 does not significantly compete for HP1 proteins in the central domain due its high preference for H3K9me3. HP1 proteins lack this large preference for H3K9me over H3K9me2 marks and are also present in a higher concentration. In the context of Suv39/Clr4^{chp1CDF61A} (mutant Clr4), the increased affinity for H3K9me2 now allows Suv39/Clr4 to engage the guided state at a majority of methylated nucleosomes, competing nonproductively with HP1 proteins.

EXPERIMENTAL PROCEDURES

Mononucleosome and Asymmetric Dinucleosome Reconstitution

Core mononucleosomes were reconstituted on the 147 bp 601 positioning sequence (Thåström et al., 1999) with or without a 5′ fluorescein label, as described previously (Canzio et al., 2011). In order to produce asymmetric dinucleosomes (N1-N2$_{K9R/MLA}$), 601 DNA fragments containing a site for the type I restriction endonuclease AarI (designed cut site CCCT) were PCR amplified, AarI digested, and assembled separately with WT, H3K9R (K9R), or H3Kc9me3 (MLA) octamers to produce N1 or N2 nucleosomes, which were ligated to produce N1-N2$_{K9R}$ or N1-N2$_{MLA}$ dinucleosomes. For detailed methods, see the Supplemental Experimental Procedures.

^{3H}SAM Incorporation Assays with Biotinylated H3$_{1–20}$ Peptides and Nucleosomes

For peptide reactions, biotinylated H3$_{1–20}$ peptide or H3$_{1–15}$ peptide effectors were produced as described previously (Canzio et al., 2011). For nucleosome reactions, 70–300 nM of core mononucleosomes or dinucleosomes were used. Reactions contained 70–100 μM cold SAM (as either chloride or iodide salt, Sigma-Aldrich) and 0.3–0.4 μM ^{3H}SAM tracer (55–75 Ci/mmol, PerkinElmer) and were incubated with varying amounts of Suv39/Clr4. Reactions were performed at 25°C in reaction buffer (RB) (100 mM Tris [pH 8.5], 100 mM KCl, 10% glycerol, 1 mM $MgCl_2$, 20 μM $ZnSO_4$, and 10 mM β-mercaptoethanol). To degrade the inhibitory reaction product S-adenosyl-homocysteine (SAH), the reaction also contained 20 μM SAH hydrolase enzyme in the case of peptide reactions. Methylation reactions were stopped by the addition of 5× SDS-loading buffer and brief incubation at 100°C. Reactions with biotinylated peptides were spotted on a SAM^2 Biotin Capture Membrane (Promega) and washed three times with 1 M NaCl and twice with ddH_20. The spots were dried and counted in a scintillation counter. Nucleosome methylation reactions were separated on 15% SDS-PAGE gels, dried, and imaged on tritium screens. Signals were visualized on a Molecular Dynamics Typhoon Imager and quantified with ImageQuant.

Quantitative Western Blots

Reactions were performed as detailed above. In biotin-tagged N1-N2$_{K9R/MLA}$ dinucleosomes (bN1-N2$_{K9R/MLA}$), reactions were stopped by the addition of 2 mM SAH and bN1-N2$_{K9R/MLA}$ captures on magnetic streptavidin beads (Dynal). Beads were washed twice in RB and bN1-N2$_{K9R/MLA}$ digested on beads with 200 U EcoR1 for 90 min at 37°C to remove N2$_{K9R/MLA}$. Beads were washed again twice with RB and resuspended in 1× SDS-loading buffer.

Reactions were separated on 4%–20% SDS-PAGE gels and transferred to a polyvinylidene difluoride membrane, blocked in 1:1 PBS:LI-COR Odssey blocking buffer (LI-COR Biosciences), and probed with H3K9me1 (monoclonal, Active Motif), H3K9me2 (monoclonal, Abcam), H3K9me3 (polyclonal, Millipore), or H4 (polyclonal, Active Motif) antisera. Signals were detected by LI-COR secondary antibodies IRDye680CW (H3K9me3 and H4) or IRDye800CW (H3K9me1 and H3K9me2). The methods employed to determine H3K9me1, H3K9me2, and H3K9me3 concentrations and extract the underlying k_1, k_2, and k_3 rate constants are described in the Supplemental Experimental Procedures.

Chromatin Immunoprecipitation

The Q-ChIP method was performed as follows: H3Kc9me1, H3Kc9me2, and H3Kc9me3 core mononucleosomes were reconstituted as detailed above and dialyzed into 50 mM HEPES (pH 7.5), 2 mM dithiothreitol, and 0.5 mM EDTA. Nucleosomes were crosslinked 15′ with 1% formaldehyde, and the reaction was quenched with 250 mM glycine. Crosslinked nucleosomes, along with a DNA standard, were separated on a native PAGE gels, stained with SyBR Gold, visualized on a Molecular Dynamics Typhoon Scanner, and quantified with ImageQuant as described previously (Canzio et al., 2011). Strain growth and chromatin preparation were performed as described previously (Canzio et al., 2011), and ChIP was performed with H3K9me-state-specific antisera (for additional details, see the Supplemental Experimental Procedures). For H3K9me1, H3K9me2, or H3K9me3 and Swi6 ChIP experiments, enrichments were plotted as the enrichment over a *clr4Δ* mutant normalized to an actin control. For Swi6 ChIP, a polyclonal antiserum was used as described previously (Canzio et al., 2011), whereas, for Chp2:7xMYC, a commercial monoclonal MYC antiserum was used (Ab32, Abcam).

Native Gel Mobility Shift Assays

Indicated concentrations of full-length WT Suv39/Clr4 were incubated with 20 nM 147 bp 601 DNA assembled WT or H3Kc9me3 mononucleosomes.

Mobility shift assays and quantifications were performed as described previously (Canzio et al., 2011).

Strain Construction

To swap the CD of Chp1 of the CD of Suv39/Clr4, we replaced the N-terminal 64 residues of Suv39/Clr4 with the N-terminal 77 residues of Chp1. The endogenous *clr4+* was replaced with either Suv39/Clr4^{W31A} or Suv39/Clr4^{chp1CDF61A} or a WT sequence and marked with a 5′ *G418^R* selectable marker flanked 5′ with 500 bp of the *clr4+* promoter. For chp2 ChIP, the endogenous *chp2+* gene was replaced with a C-terminal 7× MYC-tagged chp2 construct marked with a 3′ *Hygromycin^R* selectable marker.

SUPPLEMENTAL INFORMATION

Supplemental Information contains Supplemental Experimental Procedures and five figures and can be found with this article online at http://dx.doi.org/10.1016/j.molcel.2013.06.013.

ACKNOWLEDGMENTS

We would like to thank Shiv I.S. Grewal for the generous gift of Swi6 anitsera, Raymond C. Trievel for his generous gift of the SAH hydrolyase clone, Carrie Shiau for the production of H3Kc9me1 and H3Kc9me2 histones, Adam Larson for providing fluorescein-labeled nucleosomes, and Lindsey Pack for providing H3K9me31-15 and H3Kc9me31-15 peptides. We thank Daniele Canzio for helping to establish the initial parameters of Suv39/Clr4 methylation on peptide substrates and Jennifer Garcia for helpful comments on the Q-ChIP method. Furthermore, we thank Carol A. Gross, Jesse Zalatan, Richard S. Isaac, and Phillip Dumesic for critical reading of the manuscript and members of the Narlikar and Madhani labs for helpful comments and discussion. Research in the Narlikar lab was supported by grants from the American Cancer Society (RSG-DMC-117592), the Leukemia and Lymphoma Society, and the National Institutes of Health (NIH, GM073767). Chromatin research in the Madhani laboratory was supported by a grant from the NIH (GM071801). B.A-S. is a fellow of the Jane Coffin Childs Memorial Fund for Medical Research. B.A.-S., H.D.M., and G.J.N. designed the experiments; B.A.-S. performed all the experiments; B.A.-S., H.D.M., and G.J.N. analyzed and discussed the data; and B.A.-S., H.D.M., and G.J.N. prepared the manuscript.

Received: January 28, 2013
Revised: May 15, 2013
Accepted: June 20, 2013
Published: July 11, 2013

REFERENCES

Bhalla, K.N. (2005). Epigenetic and chromatin modifiers as targeted therapy of hematologic malignancies. J. Clin. Oncol. *23*, 3971–3993.

Bühler, M., Haas, W., Gygi, S.P., and Moazed, D. (2007). RNAi-dependent and -independent RNA turnover mechanisms contribute to heterochromatic gene silencing. Cell *129*, 707–721.

Canzio, D., Chang, E.Y., Shankar, S., Kuchenbecker, K.M., Simon, M.D., Madhani, H.D., Narlikar, G.J., and Al-Sady, B. (2011). Chromodomain-mediated oligomerization of HP1 suggests a nucleosome-bridging mechanism for heterochromatin assembly. Mol. Cell *41*, 67–81.

Carbone, R., Botrugno, O.A., Ronzoni, S., Insinga, A., Di Croce, L., Pelicci, P.G., and Minucci, S. (2006). Recruitment of the histone methyltransferase SUV39H1 and its role in the oncogenic properties of the leukemia-associated PML-retinoic acid receptor fusion protein. Mol. Cell. Biol. *26*, 1288–1296.

Ceol, C.J., Houvras, Y., Jane-Valbuena, J., Bilodeau, S., Orlando, D.A., Battisti, V., Fritsch, L., Lin, W.M., Hollmann, T.J., Ferré, F., et al. (2011). The histone methyltransferase SETDB1 is recurrently amplified in melanoma and accelerates its onset. Nature *471*, 513–517.

Cheutin, T., Gorski, S.A., May, K.M., Singh, P.B., and Misteli, T. (2004). In vivo dynamics of Swi6 in yeast: evidence for a stochastic model of heterochromatin. Mol. Cell. Biol. *24*, 3157–3167.

Couture, J.F., Dirk, L.M., Brunzelle, J.S., Houtz, R.L., and Trievel, R.C. (2008). Structural origins for the product specificity of SET domain protein methyltransferases. Proc. Natl. Acad. Sci. USA *105*, 20659–20664.

Dirk, L.M., Flynn, E.M., Dietzel, K., Couture, J.F., Trievel, R.C., and Houtz, R.L. (2007). Kinetic manifestation of processivity during multiple methylations catalyzed by SET domain protein methyltransferases. Biochemistry *46*, 3905–3915.

Elgin, S.C.R., and Grewal, S.I.S. (2003). Heterochromatin: silence is golden. Curr. Biol. *13*, R895–R898.

Fischle, W., Wang, Y.M., Jacobs, S.A., Kim, Y.C., Allis, C.D., and Khorasanizadeh, S. (2003). Molecular basis for the discrimination of repressive methyl-lysine marks in histone H3 by Polycomb and HP1 chromodomains. Genes Dev. *17*, 1870–1881.

Fritsch, L., Robin, P., Mathieu, J.R., Souidi, M., Hinaux, H., Rougeulle, C., Harel-Bellan, A., Ameyar-Zazoua, M., and Ait-Si-Ali, S. (2010). A subset of the histone H3 lysine 9 methyltransferases Suv39h1, G9a, GLP, and SETDB1 participate in a multimeric complex. Mol. Cell *37*, 46–56.

Grewal, S.I.S., and Jia, S. (2007). Heterochromatin revisited. Nat. Rev. Genet. *8*, 35–46.

Hall, I.M., Shankaranarayana, G.D., Noma, K.I., Ayoub, N., Cohen, A., and Grewal, S.I.S. (2002). Establishment and maintenance of a heterochromatin domain. Science *297*, 2232–2237.

Hong, E.J., Villén, J., Gerace, E.L., Gygi, S.P., and Moazed, D. (2005). A cullin E3 ubiquitin ligase complex associates with Rik1 and the Clr4 histone H3-K9 methyltransferase and is required for RNAi-mediated heterochromatin formation. RNA Biol. *2*, 106–111.

Horn, P.J., Bastie, J.N., and Peterson, C.L. (2005). A Rik1-associated, cullin-dependent E3 ubiquitin ligase is essential for heterochromatin formation. Genes Dev. *19*, 1705–1714.

Jencks, W.P. (1987). Binding Energy, Specificity, and Enzymic Catalysis: The Circe Effect. In Catalysis in Chemistry and EnzymologyCatalysis in Chemistry and Enzymology (New York: Dover Publications), pp. 615–797.

Jia, S.T., Noma, K., and Grewal, S.I.S. (2004). RNAi-independent heterochromatin nucleation by the stress-activated ATF/CREB family proteins. Science *304*, 1971–1976.

Jia, S., Kobayashi, R., and Grewal, S.I.S. (2005). Ubiquitin ligase component Cul4 associates with Clr4 histone methyltransferase to assemble heterochromatin. Nat. Cell Biol. *7*, 1007–1013.

Kanoh, J., Sadaie, M., Urano, T., and Ishikawa, F. (2005). Telomere binding protein Taz1 establishes Swi6 heterochromatin independently of RNAi at telomeres. Curr. Biol. *15*, 1808–1819.

Kirmizis, A., Santos-Rosa, H., Penkett, C.J., Singer, M.A., Vermeulen, M., Mann, M., Bähler, J., Green, R.D., and Kouzarides, T. (2007). Arginine methylation at histone H3R2 controls deposition of H3K4 trimethylation. Nature *449*, 928–932.

Lan, F., Collins, R.E., De Cegli, R., Alpatov, R., Horton, J.R., Shi, X., Gozani, O., Cheng, X., and Shi, Y. (2007). Recognition of unmethylated histone H3 lysine 4 links BHC80 to LSD1-mediated gene repression. Nature *448*, 718–722.

Li, H., Ilin, S., Wang, W., Duncan, E.M., Wysocka, J., Allis, C.D., and Patel, D.J. (2006). Molecular basis for site-specific read-out of histone H3K4me3 by the BPTF PHD finger of NURF. Nature *442*, 91–95.

Margueron, R., Justin, N., Ohno, K., Sharpe, M.L., Son, J., Drury, W.J., 3rd, Voigt, P., Martin, S.R., Taylor, W.R., De Marco, V., et al. (2009). Role of the polycomb protein EED in the propagation of repressive histone marks. Nature *461*, 762–767.

Munari, F., Soeroes, S., Zenn, H.M., Schomburg, A., Kost, N., Schröder, S., Klingberg, R., Rezaei-Ghaleh, N., Stützer, A., Gelato, K.A., et al. (2012). Methylation of lysine 9 in histone H3 directs alternative modes of highly dynamic interaction of heterochromatin protein hHP1β with the nucleosome. J. Biol. Chem. *287*, 33756–33765.

Nakayama, J., Klar, A.J., and Grewal, S.I. (2000). A chromodomain protein, Swi6, performs imprinting functions in fission yeast during mitosis and meiosis. Cell *101*, 307–317.

Nakayama, J., Rice, J.C., Strahl, B.D., Allis, C.D., and Grewal, S.I. (2001). Role of histone H3 lysine 9 methylation in epigenetic control of heterochromatin assembly. Science *292*, 110–113.

Narlikar, G.J., and Herschlag, D. (1998). Direct demonstration of the catalytic role of binding interactions in an enzymatic reaction. Biochemistry *37*, 9902–9911.

Noma, K., Sugiyama, T., Cam, H., Verdel, A., Zofall, M., Jia, S., Moazed, D., and Grewal, S.I. (2004). RITS acts *in cis* to promote RNA interference-mediated transcriptional and post-transcriptional silencing. Nat. Genet. *36*, 1174–1180.

Noma, K., Allis, C.D., and Grewal, S.I.S. (2001). Transitions in distinct histone H3 methylation patterns at the heterochromatin domain boundaries. Science *293*, 1150–1155.

Peña, P.V., Davrazou, F., Shi, X., Walter, K.L., Verkhusha, V.V., Gozani, O., Zhao, R., and Kutateladze, T.G. (2006). Molecular mechanism of histone H3K4me3 recognition by plant homeodomain of ING2. Nature *442*, 100–103.

Peters, A.H.F.M., Kubicek, S., Mechtler, K., O'Sullivan, R.J., Derijck, A.A.H.A., Perez-Burgos, L., Kohlmaier, A., Opravil, S., Tachibana, M., Shinkai, Y., et al. (2003). Partitioning and plasticity of repressive histone methylation states in mammalian chromatin. Mol. Cell *12*, 1577–1589.

Rea, S., Eisenhaber, F., O'Carroll, D., Strahl, B.D., Sun, Z.W., Schmid, M., Opravil, S., Mechtler, K., Ponting, C.P., Allis, C.D., and Jenuwein, T. (2000). Regulation of chromatin structure by site-specific histone H3 methyltransferases. Nature *406*, 593–599.

Reed-Inderbitzin, E., Moreno-Miralles, I., Vanden-Eynden, S.K., Xie, J., Lutterbach, B., Durst-Goodwin, K.L., Luce, K.S., Irvin, B.J., Cleary, M.L., Brandt, S.J., and Hiebert, S.W. (2006). RUNX1 associates with histone deacetylases and SUV39H1 to repress transcription. Oncogene *25*, 5777–5786.

Rice, J.C., Briggs, S.D., Ueberheide, B., Barber, C.M., Shabanowitz, J., Hunt, D.F., Shinkai, Y., and Allis, C.D. (2003). Histone methyltransferases direct different degrees of methylation to define distinct chromatin domains. Mol. Cell *12*, 1591–1598.

Sadaie, M., Kawaguchi, R., Ohtani, Y., Arisaka, F., Tanaka, K., Shirahige, K., and Nakayama, J. (2008). Balance between distinct HP1 family proteins controls heterochromatin assembly in fission yeast. Mol. Cell. Biol. *28*, 6973–6988.

Schalch, T., Job, G., Noffsinger, V.J., Shanker, S., Kuscu, C., Joshua-Tor, L., and Partridge, J.F. (2009). High-affinity binding of Chp1 chromodomain to K9 methylated histone H3 is required to establish centromeric heterochromatin. Mol. Cell *34*, 36–46.

Seeliger, D., Soeroes, S., Klingberg, R., Schwarzer, D., Grubmüller, H., and Fischle, W. (2012). Quantitative assessment of protein interaction with methyl-lysine analogues by hybrid computational and experimental approaches. ACS Chem. Biol. *7*, 150–154.

Simon, M.D., Chu, F., Racki, L.R., de la Cruz, C.C., Burlingame, A.L., Panning, B., Narlikar, G.J., and Shokat, K.M. (2007). The site-specific installation of methyl-lysine analogs into recombinant histones. Cell *128*, 1003–1012.

Tachibana, M., Ueda, J., Fukuda, M., Takeda, N., Ohta, T., Iwanari, H., Sakihama, T., Kodama, T., Hamakubo, T., and Shinkai, Y. (2005). Histone methyltransferases G9a and GLP form heteromeric complexes and are both crucial for methylation of euchromatin at H3-K9. Genes Dev. *19*, 815–826.

Thåström, A., Lowary, P.T., Widlund, H.R., Cao, H., Kubista, M., and Widom, J. (1999). Sequence motifs and free energies of selected natural and non-natural nucleosome positioning DNA sequences. J. Mol. Biol. *288*, 213–229.

Wu, H., Min, J., Lunin, V.V., Antoshenko, T., Dombrovski, L., Zeng, H., Allali-Hassani, A., Campagna-Slater, V., Vedadi, M., Arrowsmith, C.H., et al. (2010). Structural biology of human H3K9 methyltransferases. PLoS ONE *5*, e8570.

Yamada, T., Fischle, W., Sugiyama, T., Allis, C.D., and Grewal, S.I.S. (2005). The nucleation and maintenance of heterochromatin by a histone deacetylase in fission yeast. Mol. Cell *20*, 173–185.

Zhang, K., Mosch, K., Fischle, W., and Grewal, S.I.S. (2008). Roles of the Clr4 methyltransferase complex in nucleation, spreading and maintenance of heterochromatin. Nat. Struct. Mol. Biol. *15*, 381–388.

Zofall, M., Yamanaka, S., Reyes-Turcu, F.E., Zhang, K., Rubin, C., and Grewal, S.I. (2012). RNA elimination machinery targeting meiotic mRNAs promotes facultative heterochromatin formation. Science *335*, 96–100.